

Equitable Data-Driven Resource Allocation to Fight the Opioid Epidemic: A Mixed-Integer Optimization Approach

Joyce Luo and Bartolomeo Stellato

Abstract

The opioid epidemic is a crisis that has plagued the United States (US) for decades. One central issue of the epidemic is inequitable access to treatment for opioid use disorder (OUD), which puts certain populations at a higher risk of opioid overdose. We integrate a predictive dynamical model and a prescriptive optimization problem to compute the optimal locations of opioid treatment facilities and the optimal treatment budget distribution in each US state. Our predictive model is a differential equation-based epidemiological model that captures the dynamics of the opioid epidemic. We use neural ordinary differential equations to fit this model to opioid epidemic data for each state and obtain estimates for unknown parameters in the model. We then incorporate this epidemiological model for each state into a corresponding mixed-integer optimization problem (MIP) for treatment facility location and resource allocation. Our MIPs aim to minimize the number of opioid overdose deaths and the number of people with OUD, and to target socioeconomic equity by considering social vulnerability (from the US Centers for Disease Control’s Social Vulnerability Index) and opioid prescribing rates in each county. Overall, our MIPs’ proposed solutions on average decrease the number of people with OUD by $5.70 \pm 0.738\%$, increase the number of people in treatment by $21.17 \pm 3.162\%$, and decrease the number of opioid-related deaths by $0.51 \pm 0.086\%$ after 2 years compared to the baseline epidemiological model’s predictions. Rather than only evaluating the effectiveness of potential policies as in past literature, our approach is decision-focused and directly yields actionable insights for policy-makers. It provides concrete opioid treatment facility and budget allocations and quantifies the impact of these allocations on pertinent population health measures. Future iterations of this approach could be implemented as a decision-making tool to tackle the issue of opioid treatment inaccessibility.

1 Introduction

The opioid epidemic is a foremost public health crisis within the United States (US). The epidemic has been driven by increases in prescription, illicit, and synthetic opioid use, which

have in turn increased rates of opioid use disorder (OUD) and overdose deaths. According to the Centers for Disease Control (CDC), around 500,000 people have died from overdoses involving both illicit and prescription opioids from 1999 to 2019 [Centers for Disease Control, 2021c]. The COVID-19 pandemic has further exacerbated the opioid epidemic, with recent data showing a spike in overdose deaths during 2020. In the period from September 2019 through August 2020, there were 88,295 predicted deaths, which is about 27% more than the preceding 12-month period [Centers for Disease Control, 2019, Baumgartner and Radley, 2021]. The pandemic has brought to the forefront the need for expanded access to opioid addiction treatment services.

Currently, the main treatment for OUD is medication-assisted treatment (MAT), which has been proven to sustain patient recovery and prevent future overdoses. Methadone and buprenorphine are the two main medications approved to treat OUD [Amiri et al., 2020]. Methadone is administered through maintenance treatment, which requires that patients go to federally-approved facilities called opioid treatment programs (OTPs) regularly to take a prescribed amount of methadone [National Institute of Drug Abuse, 2018]. Buprenorphine is similarly used in maintenance treatment to treat OUD but can be administered by any health practitioner who obtains specialized training. This has led to a more rapid expansion of buprenorphine in comparison to methadone in the last few years. However, a recent study illustrated that methadone is still considered to be more effective at retaining patients compared to buprenorphine, especially when doses of either drug are low [Mattick et al., 2014]. Buprenorphine is also more expensive than methadone [Mattick et al., 2014]. Although access to both drugs has expanded in the last decade, there are still major gaps in access to these treatments across the US, especially in rural areas with under-developed health infrastructures. Those seeking care are often required to travel long distances to OTPs or other treatment facilities, which is another major factor that affects treatment retention [Amiri et al., 2020]. Implementing a method that proposes more equitable and concretely impactful treatment facility and budget allocations could help improve policy decision-making related to this issue.

In this work, we formulate an approach that provides optimal opioid treatment facility location and treatment budget allocation decisions to address the issue of inequitable opioid treatment facility access. Our approach integrates a dynamical model of the opioid epidemic with a prescriptive mixed-integer optimization problem (MIP) for each state. We model the state-level opioid epidemic using a ODE-based epidemiological model. In order to fit the model to real world data obtained from the CDC, National Institute on Drug Abuse (NIDA), and Substance Abuse and Mental Health Service Administration (SAMHSA), we use neural ODEs. Representing the ODE model as a neural network layer through neural ODEs allows us to exploit the power of gradient descent for more efficient parameter estimation compared to zeroth order methods [Chen et al., 2018].

We then formulate an MIP for each state to compute optimal resource allocation interventions that minimize the effect of the opioid epidemic. We do this by including a discretized version of the state-level dynamical model within the constraints of the respective state’s MIP and setting the objective to minimize overdose deaths and the number of people with

Opium Use Disorder (OUD). We capture the impact of the interventions by showing how they affect a particular parameter of our discretized epidemic model in each time period. Our approach also incorporates information about the social vulnerability of each county, which is a measure of how susceptible a community is to the adverse impacts caused by external stresses on human health [Centers for Disease Control/Agency for Toxic Substances and Disease/Geospatial Research, Analysis, and Services Program, 2021]. This information helps our MIPs target socioeconomic equitability across counties. Our MIP solutions provide concrete recommendations about how many additional treatment facilities should be in each county and how much of a limited treatment budget per time period should be allocated to each county.

1.1 Related Work

Past computational research related to the opioid epidemic has mainly centered around modeling epidemic dynamics. This research uses compartmental models, which have traditionally been used in the modeling of infectious diseases, to capture the dynamics of the opioid epidemic. The Susceptible-Infected-Recovered (SIR) model, developed by Kermack et al. [1927], is a fundamental compartmental model used in epidemiology to simulate the spread of infectious diseases such as influenza, SARS, and most recently COVID-19 [Li et al., 2022]. The SIR model uses a system of ordinary differential equations (ODEs) to model transitions between the different compartments of susceptible, infected, and recovered people within a population. A modified version of this model can be developed in regards to the opioid epidemic, as the fundamental dynamics of the opioid epidemic are similar to those of infectious diseases. Becoming addicted to opioids can be seen as analogous to being “infected” by a disease, and entering treatment for opioid addiction can be seen as entering recovery. Although these models are a simplification of the true dynamics of disease spread, they are very useful for assessing the impact of different interventions on the way the population compartments evolve over time.

White and Comiskey [2007] detail one of the first dynamical models of opiate addiction, with a focus on heroin use. Their ODE-based compartmental model gives insight into the progression of drug users, from initiation, to regular use, to addiction, to treatment, and finally, to recovery or relapse. Battista et al. [2019] expand on White and Comiskey’s compartmental model, proposing a new model based on the commonly-used Susceptible-Exposed-Infected-Recovered (SEIR) model from epidemiology. Their model specifically focuses on capturing the dynamics of the prescription opioid epidemic with four compartments: Susceptible, Prescribed, Addicted, and Rehabilitation. The transitions between each class are determined by yearly rate parameters deduced from literature or from testing ranges of parameter values [Battista et al., 2019]. We expand upon this model and other opioid epidemic compartmental modeling work by disaggregating to state level dynamics rather than national dynamics, including more population compartments, and modifying the transition dynamics.

In addition to modeling the epidemic, there is a body of literature that uses these models to project the impact of certain policy interventions on epidemic dynamics, opioid misuse, and overdose deaths. Chen et al. [2019] formulate a compartmental model of the US opi-

oid epidemic to project opioid overdose deaths under status quo conditions and subject to interventions like lowering the prescription opioid supply. Pitt et al. [2018] and Rao et al. [2021] aim to project overdose deaths, life years, and quality-adjusted life years for several different policy responses (*i.e.*, reducing opioid prescribing rates, expanding excess opioid disposal programs) using a compartmental model. The effect of a policy intervention is simulated by varying compartmental model parameters based on an “assumed magnitude” of impact and then projecting future outcomes [Pitt et al., 2018, Rao et al., 2021]. In contrast, within our approach, we directly connect specific proposed policy decisions to exact changes in our compartmental model parameter values by integrating a dynamical model of the opioid epidemic into an optimization problem. To our knowledge, no previous work takes this approach within the context of the opioid epidemic. Rather than the traditional approach of assessing the effectiveness of a broad swath of potential policies, we focus on providing a streamlined decision-making process for one type of intervention related to improving opioid treatment access.

For other applications, there have been previous efforts to integrate epidemiological models and optimization methods to inform policy decisions. Rao and Brandeau [2021] and Zaric and Brandeau [2002] use compartmental models to inform simple optimization routines that can be solved using heuristics for vaccine and budget allocation, respectively. Bertsimas et al. [2021] integrate a compartmental model of the COVID-19 pandemic, called the DELPHI model, into a prescriptive optimization problem to make decisions about the optimal locations of mass vaccination facilities and optimally allocate COVID vaccines. They formulate a bilinear non-convex optimization problem which includes a modified version of the time-discretized DELPHI model within its constraints [Bertsimas et al., 2021]. Our work builds on the DELPHI model and this framework by specializing to the opioid epidemic context. Additionally, for our compartmental model of the opioid epidemic, we take a different approach to parameter estimation by using neural ODEs. We also estimate unique model parameters for each state and formulate separate MIPs for each state, rather than having a single national-level optimization problem as in Bertsimas et al. [2021]. In doing this, our approach explicitly takes into account the unique opioid epidemic dynamics of each state, allowing for more targeted county-level solutions. Rather than only considering population-based equity, our MIPs also aim to ensure that the distribution of treatment facilities in a state is more socioeconomically equitable by considering the social vulnerability of each county.

1.2 Our Contributions

Our work has several contributions. Firstly, we seamlessly integrate a predictive dynamical model and a prescriptive optimization problem to create an operationally viable and streamlined approach for opioid treatment facility location and treatment budget allocation. This approach is novel within opioid epidemic modeling and policy-related literature. Secondly, we show that a simple neural ODE model which is informed by a dynamical structure can accurately estimate interpretable parameters from sparse time series data in the context of the opioid epidemic. These interpretable parameters can help quantify the differences

between the opioid epidemic dynamics of different states. Finally, in terms of practical contributions, we show that optimizing interventions related to opioid treatment facility location and treatment budget allocation could have a positive impact, even in the short term, on population health measures like the number of people with OUD, the number of people receiving treatment, and the number of overdose deaths. This work could help support future decision-making efforts related to improving opioid treatment access. Reproduceable code can be found here.

2 Epidemiological Model

2.1 Model Definition

We formulate a general US state-level compartmental model, partitioning the population of a state into the following 6 exhaustive population classes (compartments):

- **Susceptible (S):** Individuals who are not using opioids.
- **Prescribed (P):** Individuals who use or misuse prescription opioids but are not addicted.
- **Illicit Use (I):** Individuals who use illicit opioids like heroin.
- **Addicted (A):** Individuals who are addicted to prescription or illicit opioids.
- **Rehabilitating (R):** Individuals who are getting treatment for their addiction.
- **Deceased (D):** Individuals who have died from opioid overdoses.

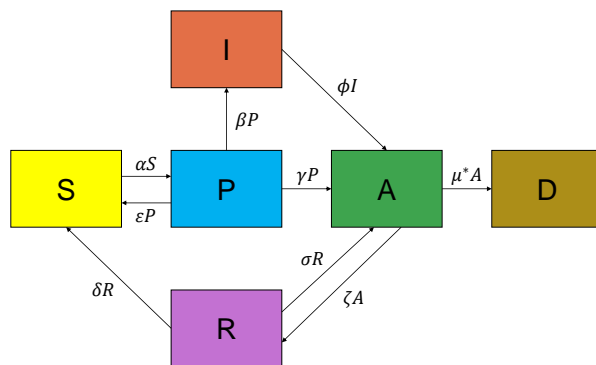


Figure 1: Flow diagram of our state-level compartmental ODE model of the opioid epidemic.

Figure 1 shows a flow diagram of the compartmental model for a particular state. The model schematic shows the different population compartments, and the arrows depict how individuals transition between these different compartments. This deterministic model can

be represented by a system of ODEs, which depends on 9 parameters. These parameters are the rates by which individuals move from one compartment to another in the model, as illustrated by their locations on particular arrows in Figure 1. We assume that each state has unique opioid epidemic dynamics and therefore a unique model parameterization.

We model the opioid epidemic using the system

$$\frac{d\mathbf{z}}{dt} = f(\mathbf{z}(t), \rho, t),$$

with state vector $\mathbf{z}(t) = (S(t), P(t), I(t), A(t), R(t), D(t)) \in \mathbf{R}^6$, and we have the initial condition $\mathbf{z}(0) = \mathbf{z}_0 = (S_0, P_0, I_0, A_0, R_0, D_0)$ consisting of estimated data for each compartment from the year 1999 for a particular US state. Vector $\rho \in \mathbf{R}^9$ represents the parameters that determine how the process evolves over time.

The dynamics are represented by the following system of ODEs:

$$\begin{aligned} \frac{dS}{dt} &= \epsilon P + \delta R - \alpha S \\ \frac{dP}{dt} &= \alpha S - (\epsilon + \gamma + \beta)P \\ \frac{dI}{dt} &= \beta P - \phi I \\ \frac{dA}{dt} &= \gamma P + \sigma R + \phi I - \zeta A - \mu A \\ \frac{dR}{dt} &= \zeta A - (\delta + \sigma)R \\ \frac{dD}{dt} &= \mu A, \end{aligned}$$

where $N = S + P + I + A + R + D$ is the total population of a particular US state. We assume that interactions between compartments are linear, as non-linear interactions were deemed negligible through parameter estimation. We estimate the unknown parameters in ρ from real world data to ensure that our dynamics function $f(\mathbf{z}(t), \rho, t)$ approximates the true dynamics as closely as possible.

2.2 Parameters

The epidemic model is based on parameters $\rho = (\alpha, \gamma, \delta, \sigma, \mu, \xi, \epsilon, \phi, \beta)$ described in Table 1. All parameters represent constant annual transition rates between particular compartments. We assume the parameters are time invariant [Battista et al., 2019]. These parameters are similar to those within previous literature [Battista et al., 2019, Pitt et al., 2018], but we add parameters which take into account the effect of illicit opioids on the dynamics of the opioid epidemic. In particular, we are interested in the illicit drug-induced addiction rate (ϕ) and how people transition from prescription to illicit opioid use (β). In a previous iteration of the model, we also considered the illicit opioid use initiation rate. However, through parameter estimation, we determined that this parameter had a negligible effect on the dynamics of

Table 1: Model parameters $\rho = (\alpha, \gamma, \delta, \sigma, \mu, \xi, \epsilon, \phi, \beta) \in \mathbf{R}^9$.

	Description
α	Prescription rate per person per year
γ	Prescription-induced addiction rate
δ	Successful treatment rate
σ	Natural relapse rate of an individual receiving treatment
μ	Death rate of addicts
ζ	Rate of individuals with OUD entering into rehabilitation
ϵ	Rate of ending prescription without addiction
ϕ	Illicit drug-induced addiction rate
β	Transition rate from prescription to illicit opioid use

the model, and it was removed. Therefore, we assume that individuals can only initiate illicit use if they previously used prescription opioids. This is also substantiated by previous research indicating that the majority of heroin users have misused prescription opioids in the past [Muhuri et al., 2013, Lankenau et al., 2012]. We set parameters $(\alpha, \gamma, \delta, \sigma) = (0.15, 0.00744, 0.1, 0.9)$ based on Battista et al. [2019] and estimate parameters $(\zeta, \epsilon, \phi, \beta, \mu)$ using our neural ODE model.

2.3 Data

We collected state-level data for the years 1999 to 2019 for compartments D , P , I , A , and R to estimate the unknown model parameters. We define the time horizon to be $H = 20$ (*i.e.*, the year 1999 represents $t = \tau = 0$ and the year 2019 represents $\tau = H$, where τ is a discrete time unit from $0, 1, \dots, H$). The Multiple Cause-of-Death dataset in the CDC WONDER (Wide-ranging Online Data for Epidemiologic Research) database [Centers for Disease Control, 2019] was our source for yearly overdose death counts (D) from 1999–2019. To identify opioid-specific deaths, we filtered the dataset using the multiple cause-of-death (ICD) codes for heroin (T40.1), natural opioid analgesics (T40.2), methadone (T40.3), and synthetic opioid analgesics other than methadone (T40.4). We also used underlying cause-of-death codes X40–X44 (unintentional), X60–X64 (suicide), and Y10–Y14 (undetermined) [Centers for Disease Control, 2021a]. The CDC suppresses data values below a threshold of 10 to prevent patient identification, so we removed states if over 20% of their data was suppressed. The following states were removed: North Dakota, South Dakota, Alaska, Idaho, Montana, Mississippi, Wyoming, and West Virginia. For states with fewer suppressed measures, these were replaced with a random number between 1 and 9 drawn from a uniform distribution. We made the deaths cumulative, starting from the number of opioid-related deaths in 1999. This is because we assume that the Deceased compartment is absorbing, since those who die from opioid overdoses cannot transition into other compartments.

We approximated the number of people using prescription opioids per year per state (P) using data sources from the CDC. The CDC provides data regarding opioid dispensing rates for each state from 2006 to 2019 [Centers for Disease Control, 2021b]. We used this data to calculate ratios of the number of prescription opioids dispensed in each state to the number dispensed nationally. In addition, the CDC’s National Health and Nutrition Examination Survey (NHANES) provides biyearly estimates of the percentage of adults nationwide who used a prescription opioid in the past 30 days for the years 1999–2018 [Centers for Disease Control, National Center for Health Statistics, 2019]. From these percentages, we estimated the *number* of adults nationwide who used a prescription opioid per year. To obtain state-level estimates, we multiplied our state-to-national ratios by the nationwide estimate calculated from NHANES for each year from 2006–2018.

From SAMHSA’s National Survey on Drug Use and Health (NSDUH), we obtained data on the yearly prevalence of OUD (A) for each state from 2016–2019. We also obtained the yearly estimated number of heroin users for each state from 2016–2019 (I) [U.S. Department of Health and Human Services, Substance Abuse and Mental Health Services Administration, Center for Behavioral Health Statistics and Quality, 2019]. For the number of people in treatment (R), we obtained data from the National Survey of Substance Abuse Treatment Services (N-SSATS) for the years 2000, 2002–2013, 2015–2017, and 2019 [U.S. Department of Health and Human Services, Substance Abuse and Mental Health Services Administration, Center for Behavioral Health Statistics and Quality, 2021]. The data measure was the aggregated number of clients receiving MAT across all facilities in a state within a day each year.

We calculated the number of susceptible people (S) based on data from the other 5 compartments and the populations of each US state. We assume that $N^{(\tau)} = S^{(\tau)} + P^{(\tau)} + I^{(\tau)} + A^{(\tau)} + R^{(\tau)} + D^{(\tau)}$, where $N^{(\tau)}$ is the state population in year τ . The death counts are included in this summation because they are negligible compared to the total population. We implicitly consider overall birth and death rates of the population by allowing $N^{(\tau)}$ to vary. We calculated the S compartment only for the time points with complete data for all other compartments. For other time points, the S value was set to 0. We detail how we set the model initial conditions in Appendix A.

We created data matrices for every included US state. Each data matrix is 21×6 , and each row represents $\mathbf{z}^{(\tau)}$, the data observation at time $t = \tau$ for $\tau = 0, 1, \dots, H$. Since there are 6 different compartments, $\mathbf{z}^{(\tau)}$ lives in \mathbf{R}^6 . Missing compartment values were set to 0. In order to ensure convergence and a better model fit, we normalized each compartment’s value by $N^{(\tau)}$ at each time point.

2.4 Neural ODE Model

The neural ODE framework represents ODEs and their solvers as a neural network layer, which is called a neural ODE layer in Chen et al. [2018]. ODEs and ODE solvers fit perfectly into the neural network framework, as they have been proven to be differentiable [Chen et al., 2018]. Using this neural ODE framework, we are able to estimate unknown parameters of our ODE-based models by training a simple neural network. We construct a single-layer

neural ODE model, where the layer is defined by the ODEs of our compartmental model (described in Section 2.1). We use gradient-based optimizers to minimize the following loss function:

$$\mathcal{L}(\rho) = \sum_{\tau=0}^H \ell(\hat{\mathbf{z}}^{(\tau)}, \mathbf{z}^{(\tau)}),$$

where $\hat{\mathbf{z}}^{(\tau)}$ is the ODE model’s prediction of the vector of compartment values and $\mathbf{z}^{(\tau)}$ is our observation of the vector of compartment values from the data at time $t = \tau$ for $\tau = 0, 1, \dots, H$. The vectors $\hat{\mathbf{z}}^{(\tau)}$ and $\mathbf{z}^{(\tau)}$ lie in \mathbf{R}^6 . Our neural ODE model minimizes the distance between $\hat{\mathbf{z}}^{(\tau)}$ and $\mathbf{z}^{(\tau)}$ by varying the parameters ρ . We define:

$$\ell(\hat{\mathbf{z}}^{(\tau)}, \mathbf{z}^{(\tau)}) = \|q_{\tau} \odot (\hat{\mathbf{z}}^{(\tau)} - \mathbf{z}^{(\tau)})\|_2^2,$$

where $q_{\tau} \in \mathbf{R}^6$ is defined to accordingly penalize differences between the predictions and observations based on data availability at time point τ . For instance, if there is no data for a compartment at τ , the corresponding element in q_{τ} is set to 0 and the data element is ignored in the loss calculations. However, if the rest of the data at τ is available, the corresponding elements in q_{τ} are set to 1 and only those elements are used to calculate the loss. Here, \odot denotes the element-wise product of q_{τ} and $\hat{\mathbf{z}}^{(\tau)} - \mathbf{z}^{(\tau)}$.

In contrast to traditional neural networks, the neural ODE framework does not require a large amount of data to estimate parameters accurately, which makes it ideal for applications with limited data like is the case for the opioid epidemic. It also allows us to estimate parameters in a more computationally efficient way, because we are able to estimate the parameters based on the direction of the gradient [Chen et al., 2018].

Implementation. We use Julia to implement our neural ODE model. In particular, we use the `DiffEqFlux.jl` [Rackauckas et al., 2019] and `DifferentialEquations.jl` [Rackauckas and Nie, 2017] libraries. We train our neural ODE model using this method for each individual state. Our initial condition is a vector of the normalized compartment values in 1999 for each respective state. We set an initial guess for the unknown parameters: $(\phi, \epsilon, \beta, \zeta, \mu) = (0.3, 0.9, 0.19, 0.5, 0.01159)$, according to parameter ranges and estimates from previous literature [Battista et al., 2019]. We restrict the parameters to be non-negative by representing them as the square of the actual parameters we estimated (*e.g.*, $\phi = \hat{\phi}^2$, where $\hat{\phi}$ is the actual Neural ODE parameter that we learn). We use the ODE solver `Tsit5` and the `ForwardDiffSensitivity` method to calculate the gradients. To perform stochastic gradient descent, we run the ADAM optimization algorithm for 20000 iterations with a step size of 0.0001, followed by the BFGS algorithm.

3 Mixed-Integer Optimization Problem

The overarching goal of our approach is to offer solutions to ensure that MAT and treatment facilities are more accessible and allocated equitably. Accordingly, for each US state, we formulate a prescriptive MIP to address two main objectives: opioid treatment facility location

and treatment budget allocation. In particular, we focus on treatment facilities that offer MAT. Our MIPs mainly aim to minimize overdose deaths and the number of people with OUD, but also take into account socioeconomic considerations so that treatment facilities are distributed more equitably. The initial starting point for our problem is 2017, as that year has sufficient data availability. We set our modeling period to be 2 years.

3.1 Data

We obtained data related to the current number of treatment facilities that offer MAT in each county, using the SAMHSA Behavioral Health Treatment Services Locator. This tool helped us create a dataset that indicated the number of treatment facilities that offered “Outpatient methadone/buprenorphine or naltrexone treatment” in each county [Substance Abuse and Mental Health Services Administration, 2022]. We needed this data to account for the effect of facilities that are already treating patients with MAT. We also obtained data from the CDC’s Social Vulnerability Index (SVI), which provides a value for each county that captures 15 factors from the US Census, including poverty, lack of vehicle access, and crowded housing [Centers for Disease Control/Agency for Toxic Substances and Disease/Geospatial Research, Analysis, and Services Program, 2021]. This index is intended to help identify populations that are vulnerable during public health emergencies like the opioid epidemic. The SVI ranking is a value between 0 and 1, with a ranking closer to 1 indicating that the region is more socially vulnerable [Centers for Disease Control/Agency for Toxic Substances and Disease/Geospatial Research, Analysis, and Services Program, 2021]. The CDC provides SVI data every 2 years, and we obtained county-level data for 2018. Additionally, we obtained county-level data regarding opioid dispensing/prescribing rates per 100 people for 2018 [Centers for Disease Control, 2021b] and county population totals from the Census Bureau [United States Census Bureau, 2021].

Budgetary information for each state was obtained for the constraints of our MIPs. We obtained total grant funding data for each state in 2018 from the US Department of Health and Human Services Opioid Grants Dashboard [U.S. Department of Health and Human Services, 2020]. According to previous opioid grant spending analyses, around 65% of grant funding was used for treatment initiatives in a particular year [Murrin, 2020]. In addition, the estimated cost of opening a treatment facility ranges from \$300–600K for an intensive outpatient facility [Ascension Recovery Services, 2019]. We rounded up the cost to \$1,000,000 to have a higher estimate. For each state, we budgeted 65% of the total grant funding to be used for opening new treatment facilities and divided this number by \$1,000,000 to get the maximum *additional* number of treatment facilities that can be opened in that state. We added this number to the current number of treatment facilities to get cap on the number of facilities that can be opened in that state, which we call N .

SAMHSA recently distributed a grant to states for the purposes of expanding MAT [Murrin, 2020]. We divided the amount distributed to each state by 4 to get quarterly estimates of the treatment budget, which we call d_k at time k . For the scope of this work, we chose to only focus on methadone-based MAT. Accordingly, we also obtained data on the cost of treating a patient with methadone-based MAT, which was \$37.38 [Centers for Medicare and

Medicaid Services, 2021]. Multiplying this number by 12 gave us $d = \$448.56$, the quarterly cost of methadone-based MAT. In future iterations of this MIP, we could additionally take into account buprenorphine-based MAT.

3.2 Problem Formulation

We consider an optimization problem over a time horizon K with time periods $k \in \mathcal{K} = \{1, \dots, K\}$. We denote each county in a state as i with $i \in \mathcal{C} = \{1, \dots, C\}$, where C is the total number of counties in a state. The decision variables are x_i —denoting the number of opioid treatment facilities with MAT needed for county $i \in \mathcal{C}$, and \bar{d}_{ik} —denoting the treatment budget distributed to county $i \in \mathcal{C}$ at time $k \in \mathcal{K}$. The optimization problem will feature the parameters in Table 2.

Table 2: Parameters of the optimization problem.

	Description
n_i	Number of opioid treatment facilities with MAT already in county $i \in \mathcal{C}$
SVI_i	Social Vulnerability Index in county $i \in \mathcal{C}$
pr_i	Prescribing rate per 100 people in county $i \in \mathcal{C}$
Pop_i	Population in county $i \in \mathcal{C}$
N	Maximum number of treatment facilities that can be open in the state
d_k	Treatment budget limit for time $k \in \mathcal{K}$
d	Quarterly per patient cost of MAT
α	Prescription rate per person per year
γ	Prescription-induced addiction rate
δ	Successful treatment rate
σ	Natural relapse rate of an individual in treatment
μ	Death rate of addicts
ζ	Rate of individuals with OUD entering into rehabilitation
ϵ	Rate of ending prescription without addiction
ϕ	Illicit drug-induced addiction rate
β	Transition rate from prescription to illicit opioid use

To use the continuous time compartmental model described in Section 2.1 within the constraints of our optimization problem, we discretize it using the forward Euler method [Willcox and Wang, 2014]. We set $t = k\Delta$, where Δ is the time discretization interval and $k \in \mathcal{K}$. In order to mimic the continuous time trajectory as closely as possible while also not making Δ too small, we set $\Delta = 0.25$. This represents a time increment of 3 months.

Our decision variables regarding opening additional treatment facilities and establishing treatment budgets for counties act as proposed interventions that affect state-level opioid epidemic dynamics. The effect of interventions in the system can be shown by changing related compartmental model parameters [Pitt et al., 2018, Rao et al., 2021]. We model the impact of our decision variables on state-level opioid epidemic dynamics by showing how they affect the estimated parameter ζ in each time period. We choose to affect ζ because it represents the transition rate from the A to R compartment. Having greater access to opioid treatment facilities that offer MAT helps more people who have OUD get the treatment they need. Therefore, optimizing the treatment facility distribution and treatment budget allocation should increase the transition rate from A to R . We specifically affect ζ based on the proportion of extra people that could transition from the A to R compartment if a certain number of new treatment facilities offering MAT were established. We define this proportion as

$$\ell_k = \frac{\sum_{i=1}^C (x_i - n_i) \bar{d}_{ik} / dx_i}{A_k},$$

which is added to ζ in each time period. Here, \bar{d}_{ik} / dx_i represents the number of patients treated per facility per time increment and depends on two of the decision variables. The numerator of ℓ_k represents the additional number of people who could be treated in the state due to the new treatment facilities. We then divide this number by A_k to get the added rate of transition from the A to R compartments. For a particular state, we have the following dynamics:

$$\begin{aligned} S_{k+1} &= S_k + (\epsilon P_k + \delta R_k - \alpha S_k) \Delta \\ P_{k+1} &= P_k + (\alpha S_k - (\epsilon + \gamma + \beta) P_k) \Delta \\ I_{k+1} &= I_k + (\beta P_k - \phi I_k) \Delta \\ A_{k+1} &= A_k + (\gamma P_k + \sigma R_k + \phi I_k - (\zeta + \ell_k) A_k - \mu A_k) \Delta \\ R_{k+1} &= R_k + ((\zeta + \ell_k) A_k - (\delta + \sigma) R_k) \Delta \\ D_{k+1} &= D_k + (\mu A_k) \Delta. \end{aligned}$$

Collectively, we call this dynamics function \bar{f} since this is our approximated compartmental dynamics function with estimated model parameters (one parameter of which is affected by our decision variables). For a particular US state, we define the following treatment facility location and budget allocation problem:

$$\begin{aligned} \text{minimize} \quad & D_K + \lambda_A \sum_{k=0}^K (A_k) + \lambda_{\text{pr}} \psi_{\text{pr}}(\mathbf{x}) + \lambda_{\text{SVI}} \psi_{\text{SVI}}(\mathbf{x}) + \lambda_{\text{Pop}} \psi_{\text{Pop}}(\bar{\mathbf{d}}_k) \\ & + \lambda_{\text{inf}} \max\left(0, \sum_{i=1}^C x_i - N\right) \\ \text{subject to} \quad & x_i \geq n_i, \quad \forall i \in \mathcal{C} \\ & \sum_{i=1}^C \bar{d}_{ik} \leq d_k, \quad \forall k \in \mathcal{K} \\ & \mathbf{z}_{k+1} = \bar{f}(\mathbf{z}_k, \mathbf{x}, \bar{\mathbf{d}}_k), \quad k = 1, \dots, K-1 \\ & x_i \in \mathbf{Z}, \quad x_i \geq 1, \quad \forall i \in \mathcal{C} \\ & \mathbf{z}_k = (S_k, P_k, I_k, A_k, R_k, D_k) \geq 0, \quad \forall k \in \mathcal{K} \\ & \bar{d}_{ik} \geq 0, \quad \forall i \in \mathcal{C}, k \in \mathcal{K}. \end{aligned}$$

Objective. Within the MIP objective function, we prioritize minimizing the total number of overdose deaths and the number of people with OUD, which are the first two terms of the objective. In the next two terms, we minimize the 1-norm distance between \mathbf{x} , which is a vector of decision variables for the number of treatment facilities in every county, and the ideal distribution of treatment facilities based on the prescribing rates (vector \mathbf{pr}) or SVI rankings (vector \mathbf{SVI}) of each county. We define these functions as $\psi_{\mathbf{pr}}(\mathbf{x}) = \|\mathbf{x} - N \cdot \mathbf{pr} / (\sum_{i=1}^C \text{pr}_i)\|_1$ and $\psi_{\mathbf{SVI}}(\mathbf{x}) = \|\mathbf{x} - N \cdot \mathbf{SVI} / (\sum_{i=1}^C \text{SVI}_i)\|_1$, respectively. The parameters $\lambda_{\mathbf{pr}}$ and $\lambda_{\mathbf{SVI}}$ determine whether the distribution of treatment facilities is closer to the prescribing rate distribution or the SVI ranking distribution. These terms ensure that the distribution of treatment facilities is more equitable. In the fifth term, we penalize the difference between the ideal treatment budget distribution based on county population (vector \mathbf{Pop}) and our MIP’s treatment budget allocation in each time period (vector $\bar{\mathbf{d}}_k$). We define this function as $\psi_{\mathbf{Pop}}(\bar{\mathbf{d}}_k) = \|\bar{\mathbf{d}}_k - d_k \cdot \mathbf{Pop} / (\sum_{i=1}^C \text{Pop}_i)\|_\infty$. We set the following hyperparameters: $\lambda_A = 0.9$, $\lambda_{\mathbf{pr}} = 0.3$, $\lambda_{\mathbf{SVI}} = 1 - \lambda_{\mathbf{pr}}$, and $\lambda_{\mathbf{Pop}} = 0.1$. λ_{inf} is adjusted for each state, which is described in Appendix C. The final term of the objective function is essential for solution feasibility. In most cases, $\sum_{i=1}^C x_i = N$, as we aim to cap the total number of treatment facilities in the state at N . If $\sum_{i=1}^C x_i \geq N$, this indicates that the state’s solution must be over budget to be feasible. In order to minimize the amount that a solution is over budget, we penalize $\sum_{i=1}^C x_i - N$ by setting a large λ_{inf} . This objective function approach gives us more insight into potential solutions if particular states exceed their budget.

Constraints. The first constraint ensures that the optimal number of treatment facilities in a county is greater than or equal to the number of treatment facilities already in that county. The second constraint limits the sum of the treatment budgets distributed to each county by the state treatment budget limit for time k . The third constraint describes the discretized compartmental model for the particular state. The fourth constraint restricts the x_i ’s to be integer-valued and requires that there is at least one treatment facility in each county. This ensures that there will not be any issues with dividing by 0, as we divide by x_i within our ℓ_k term. The fifth constraint describes the domain of the compartment values at each time k , and the sixth constraint similarly describes the domain of the \bar{d}_{ik} decision variables. The problem as shown here is not easily solved by a numerical MIP solver, since we are dividing two decision variables within ℓ_k and have a non-convex objective. We reformulate the problem to have at most quadratic constraints and a linear objective, which is shown in Appendix B.

Implementation. We use the Gurobi Optimizer to solve the optimization problem for each state. The Gurobi 10.0 bilinear solver can handle non-convex quadratic constraints in a mixed-integer programming context. We implement each state MIP with the `JuMP.jl` mathematical optimization framework in Julia [Dunning et al., 2017]. We set the parameter `NonConvex` to 2. Depending on the size of the optimization problem, we also set the `TimeLimit` parameter to 2000 seconds to prioritize the solver finding a good feasible solution rather than an optimal solution. Reproduceable code can be found here.

4 Results and Discussion

4.1 Epidemiological Model Parameter Estimation using Neural ODEs

Figure 2 shows the estimated parameters from our neural ODE model for each US state. The exact parameter values are included in Appendix D. Figure 2 illustrates that the ϕ and β parameters seem to be correlated. In addition, they tend to be approximately 0 for many of the states. Both parameters have to do with illicit opioid use, which is likely why they are correlated for each state. We also hypothesize that the parameter values are negligible for many states because the NDSUH surveys tend to underestimate the prevalence of illicit opioid use in particular. However, for states where these parameters are non-negligible, we can interpret them. For New York, we see that $\phi = 0.05511$, which implies that around 5 in 100 New Yorkers who use illicit opioids will develop OUD. This rate is higher than the prescription-induced addiction rate $\gamma = 0.00744$, which we set based on previous literature. This makes sense because illicit opioids like heroin tend to be more addictive than prescription opioids. We see that $\beta = 0.005029$ for New York, which means that around 5 in 1000 New Yorkers who are using prescription opioids will begin using illicit opioids within a year. This seems to align with estimates which state that around 4–6% of individuals who misuse prescription opioids transition to heroin [National Institute on Drug Abuse, 2021]. Since our P compartment also includes people who properly use prescription opioids, it makes sense that our parameter estimate would be smaller. Notably, Vermont has the largest ϕ and β parameters, which means they have the highest illicit addiction rate and highest transition rate from prescription to illicit opioids. This could be the result of Vermont having better data quality than other states related to illicit opioid use. However, it could also be indicative that Vermont has a problem with people transitioning from prescription to illicit opioid use and becoming addicted. More states have non-negligible β parameters compared to ϕ parameters, which means that the transition between prescription opioid use and illicit use is a contributing factor to the state-level opioid epidemic.

The other parameters μ , ζ , and ϵ are consistently non-negligible across all states. The death rate of addicts μ is similar in magnitude to previous calculated death rates. For instance, Battista et al. [2019] calculate the death rate of addicts to be 0.01159, which we use as our initial guess for μ . After training, our μ parameter is still around this value for all states. The states with the highest death rate of addicts are Oklahoma (0.02198) and New Mexico (0.02149) according to our parameter estimation. The rate of entry into rehabilitation ζ is also within the approximate range determined by Battista et al. [2019] which was 0.2–2. Our estimated ζ values are within the range 0.1–0.52, with Maryland having the largest ζ value. A ζ value of 0.2 means that 20 addicted people enter treatment out of 100 addicted people. The rate of ending prescription without addiction per prescription user and year ϵ is also within the range 0.8–8 determined by Battista et al. [2019]. Battista et al. determine this parameter range based on a study conducted by Shah et al. [2017] which shows that the time individuals spend using prescription opioid ranges from 1 month to 3 years. The estimated ϵ values range from 1–4 for different states, indicating that most

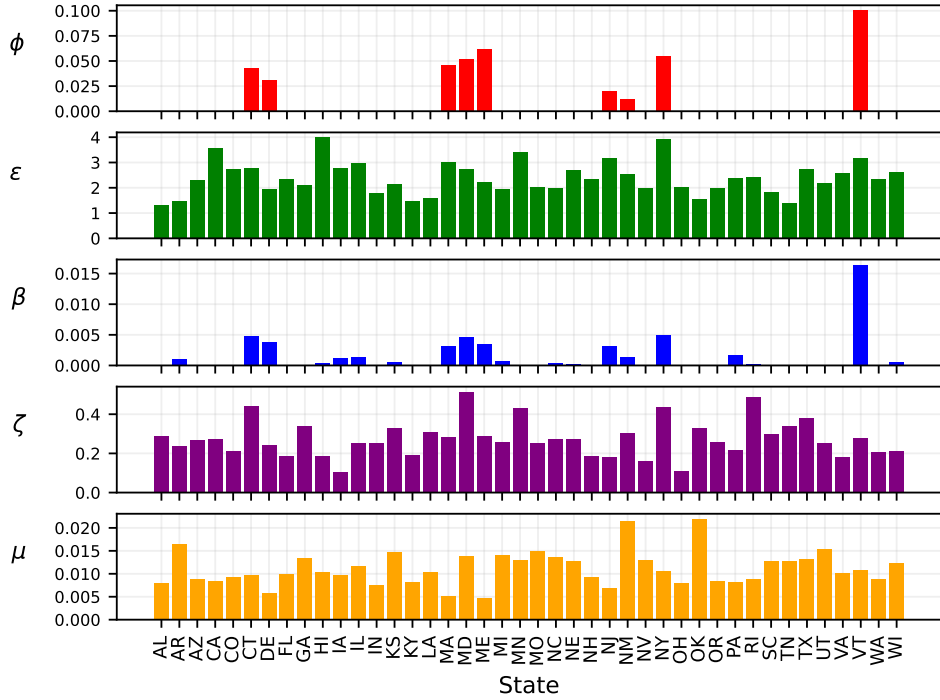


Figure 2: Estimated parameters for each US state.

patients are ending their prescriptions without addiction within a year. Hawaii and New York have the largest ϵ values which means that patients end their prescriptions without addiction faster.

4.2 Epidemiological Model Validation

Figure 3 illustrates the neural ODE model predicted dynamics in comparison to the actual population proportion values for the compartments P , I , A , R , and D from 1999–2019 for New York. The model captures the steady increase in the D proportion values and the slight increase over the years in the R proportion values. For the I compartment, the data shows a slight decrease in the proportion of heroin users from 2016–2019, but an overall slight increase since 1999. Our model is linear, so it is only able to capture the slight increase in the I proportion values since 1999. If we were able to incorporate fentanyl use data, there would likely have been a larger increase in the I proportion values. For the A compartment, the model predicts that the proportion of people with OUD has been increasing since 1999, which fits with the data. Since the data is sparse, the model does not capture the slight decrease from 2018–2019. Compared to the other compartments, a much larger proportion of the population is captured within the P compartment, since many people are prescribed prescription opioids for pain but are not abusing them. The model captures the drastic increase in opioid prescriptions which occurred in the 1990s as doctors began to prescribe opioids to many more patients. The trend in the proportion of prescription opioid users has

since flattened and slightly decreased, which the model captures as well. The loss progression throughout training is shown in Appendix D.

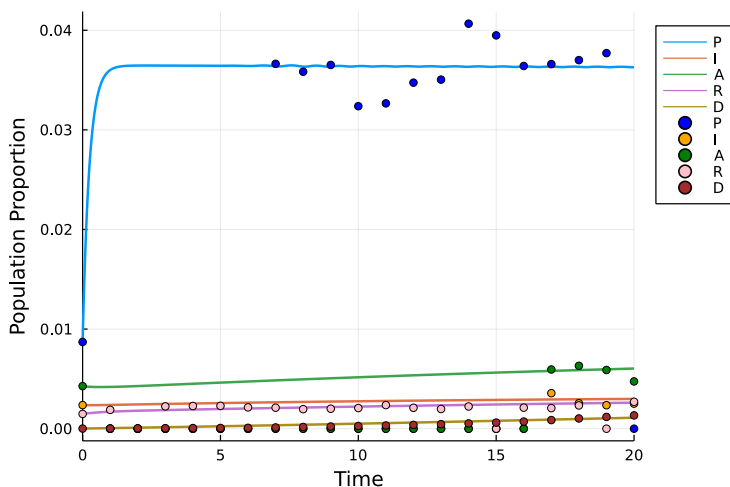
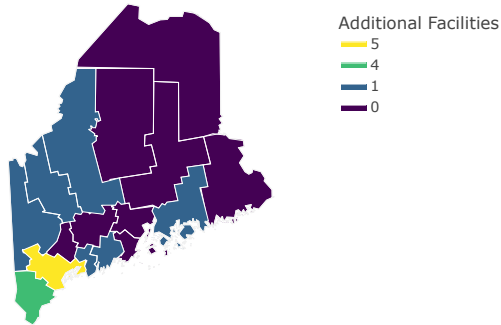


Figure 3: Neural ODE model predictions in comparison to the actual population proportion values in each year from 1999–2019 for New York.

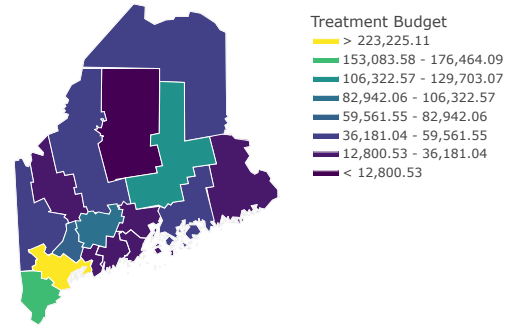
4.3 Optimization Problem Solutions

We obtain solutions for the majority of US states from our MIPs, which give the treatment facility and treatment budget distributions across counties in each state. Figure 4 shows the additional treatment facilities and treatment budget distributions determined by the MIP solutions for 4 states: Maine, California, Indiana, and Florida. We display the solution of one state from each main geographic region (Northeast, West, Midwest, and South). The MIPs for Maine and Indiana have optimal solutions, and the MIPs for California and Florida have feasible solutions. Figures 4a, 4c, 4e, and 4g show that most counties in each state either do not need any additional treatment facilities or only need one additional facility to be opened. There is one main county in each state that requires more additional treatment facilities than the others. The solution to the California MIP (shown in Figure 4c) recommends that there should be 43 additional treatment facilities in Los Angeles county. California has more grant funding in comparison to other states, which is why they can afford to add 43 additional treatment facilities to a particular county. For Maine, Indiana, and Florida, the counties with the greatest number of recommended additional treatment facilities are Cumberland, Marion, and Miami-Dade, respectively. These counties also have the greatest population in each corresponding state. Nevertheless, we can still see that incorporating the social vulnerability and prescribing rate in each county had some effect on making the solutions more equitable.

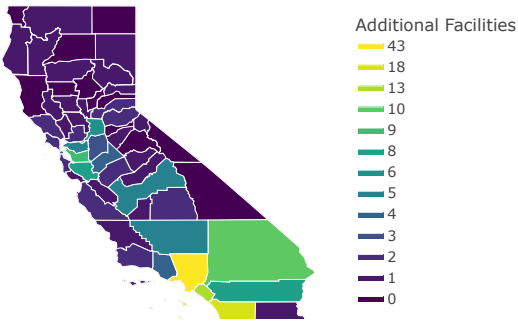
As an example, Figure 5 shows the Florida treatment facilities solution in comparison to the SVI rankings and prescribing rate distributions. We set $\lambda_{pr} = 0.3$ and $\lambda_{SVI} = 0.7$



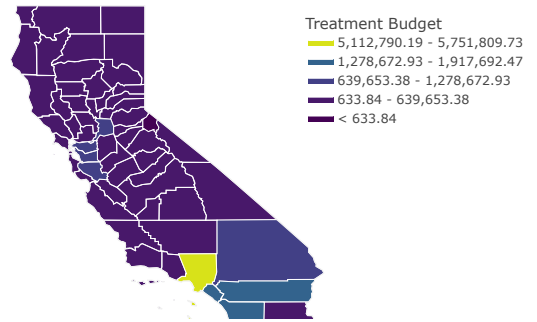
(a) ME Additional Facilities Distribution



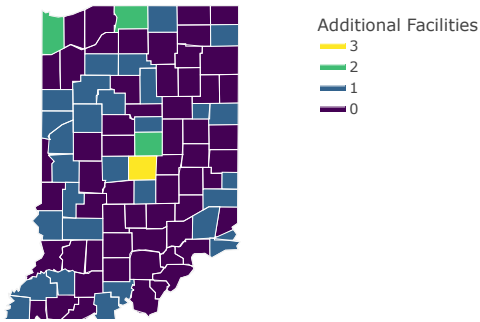
(b) ME Treatment Budget Distribution



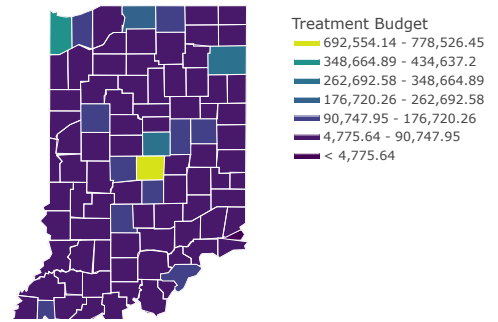
(c) CA Additional Facilities Distribution



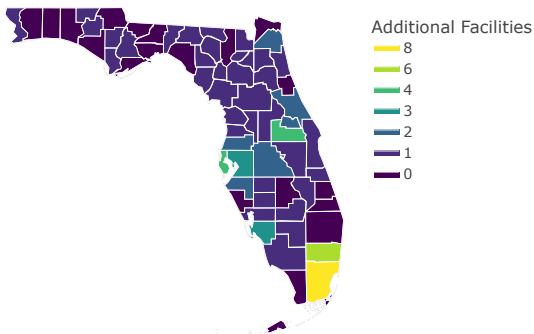
(d) CA Treatment Budget Distribution



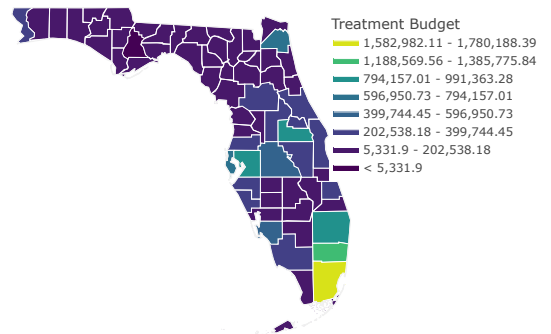
(e) IN Additional Facilities Distribution



(f) IN Treatment Budget Distribution



(g) FL Additional Facilities Distribution



(h) FL Treatment Budget Distribution

Figure 4: State MIP solutions consisting of additional facilities and treatment budget distributions.

so that the MIP prioritizes its treatment facility solution to be closer to the SVI ranking distribution rather than the prescribing rate distribution. The recommended number of treatment facilities per county in Figure 5c more closely matches up with the high SVI ranking counties in Figure 5a compared to the high prescribing rate counties in Figure 5b. The recommended number of treatment facilities in a county is not exactly proportional to the SVI ranking because some counties already have more initial treatment facilities due to their population sizes. In addition, the MIP prioritizes minimizing deaths and the number of people with OUD when allocating facilities. However, comparing Figure 4g and Figure 5a, we can see that at least 1 additional facility is recommended for most counties with notably higher SVI rankings. Overall, our solutions are more equitable because we are able to incorporate these factors into our MIPs.

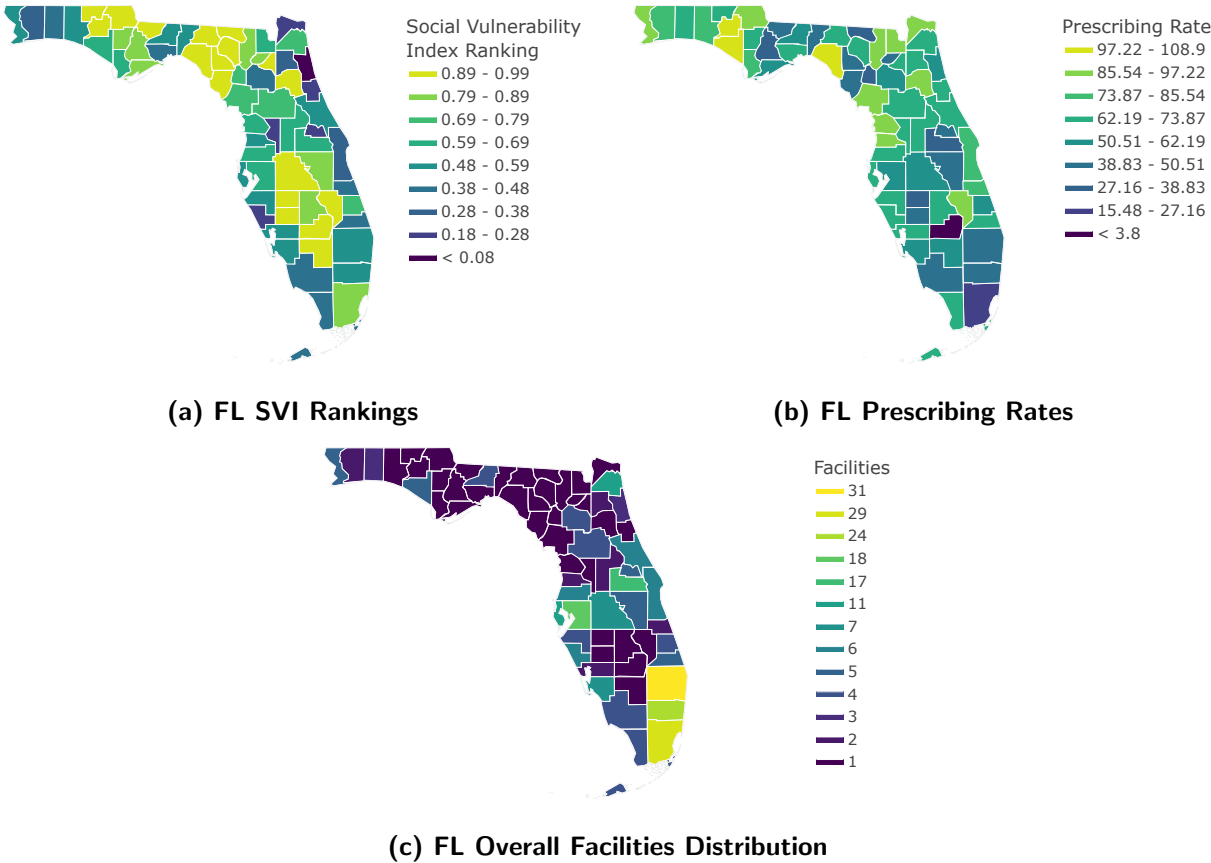


Figure 5: Comparison between the SVI rankings distribution, the prescribing rate distribution, and the treatment facilities distribution determined by the Florida MIP solution.

Figures 4b, 4d, 4f, and 4h show the treatment budget distributions yielded by the MIP solutions for Maine, California, Indiana, and Florida in a given three month time frame. For each state, the recommended budget distributions are the same for every 3 month interval within our modeling period. We want the treatment budget distribution to be as close to the population distribution as possible, in order to distribute larger treatment budgets to

counties with larger populations. Accordingly, our solutions distribute the largest portion of each state’s treatment budget to counties with the largest populations in each state—Cumberland, Los Angeles County, Marion, and Miami-Dade, respectively.

Solution Impact. Table 3 quantifies the effect of optimizing the locations of additional treatment facilities and the treatment budget allocation on the compartments A , R , and D after 2 years for almost all US states. In comparison to our baseline compartmental model predictions, the proposed solutions to the respective state MIPs on average decrease the number of people with OUD by $5.70 \pm 0.738\%$, increase the number of people getting treatment by $21.17 \pm 3.162\%$, and decrease the number of opioid-related deaths by $0.51 \pm 0.086\%$ after 2 years (Figure 6).

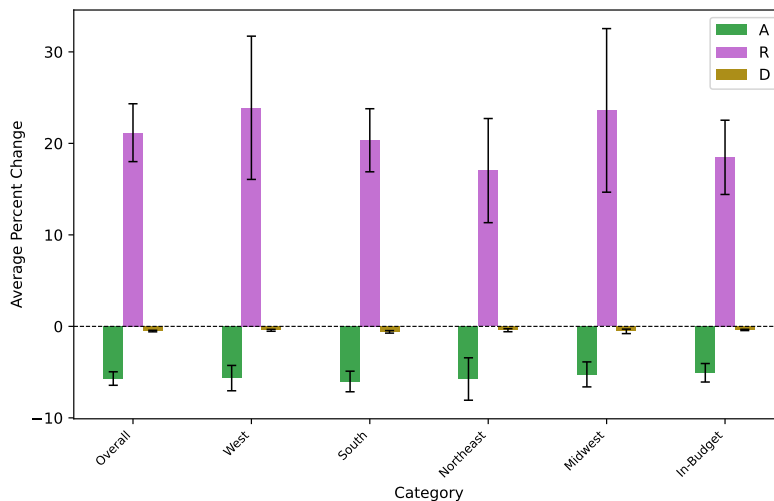


Figure 6: Average effect of our MIP solutions on compartments A , R , and D for various solution groupings.

Figure 6 additionally shows the average effect of the MIP solutions on compartments A , R , and D for the main US geographic regions: Northeast, West, Midwest, and South. From Table 3, we see that Rhode Island has the greatest percentage decrease in the number of people with OUD at -13.66% . Iowa has the greatest percentage increase in the number of people receiving treatment at 50.3% . Nebraska has the greatest percentage decrease in opioid-related deaths at -1.55% . Across states, our MIP solutions have the greatest impact on the number of people in rehabilitation (R) because our decision variables directly affect the parameter ζ , which dictates how the R compartment evolves over time.

Within Table 3, we also differentiate between whether the state MIP yields an optimal solution, a feasible solution within a time limit, or an over budget solution. States with no symbols within the table have MIPs that yielded an optimal, within-budget solution. For states like Texas, North Carolina, and Florida, Gurobi only found a feasible solution within the time limit because those states have a large number of counties, which adds to the complexity of the MIP. There were only 10 states for which Gurobi was not able to certify

Table 3: Effect of our state MIP solutions on the values of compartments A , R , and D in comparison to baseline opioid epidemic dynamics after 2 years (in percentages).

State	A	R	D
AL†	-8.07	26.92	-1.05
AR†	-5.13	22.53	-0.78
AZ	-5.14	18.05	-0.37
CA*	-8.3	28.06	-0.57
CO	-4.98	23.04	-0.35
CT	-3.22	6.46	-0.24
DE	-3.67	12.78	-0.34
FL*	-4.17	21.37	-0.32
GA†	-6.25	17.61	-0.63
HI	-9.32	47.03	-0.7
IA†	-5.58	50.3	-0.64
IL	-2.44	9.03	-0.21
IN	-3.13	11.96	-0.31
KS†	-7.18	21.28	-0.77
KY†	-4.81	23.27	-0.35
LA†	-8.66	27.76	-1.01
MA*†	-4.53	13.63	-0.26
MD*	-5.68	9.56	-0.47
ME	-1.96	5.78	-0.12
MI	-4.88	18.43	-0.49
MN†	-5.87	12.58	-0.51
MO†	-4.95	19.35	-0.4
NC*	-3.38	11.47	-0.33
NE†	-9.94	36.35	-1.55
NH	-5.86	25.24	-0.48
NJ*†	-3.51	17.26	-0.24
NM†	-6.18	17.73	-0.55
NV†	-6.31	38.72	-0.53
NY*	-4.07	8.49	-0.3
OH*	-5.47	43.08	-0.33
OK†	-9.42	28.41	-0.89
OR	-4.02	14.89	-0.3
PA*	-6.52	26.92	-0.55
RI	-13.66	24.12	-0.65
SC	-3.79	12.4	-0.41
TN†	-9.26	27.16	-0.66
TX*†	-7.33	19.34	-0.77
UT	-2.82	10.86	-0.2
VA†	-4.7	24.17	-0.39
VT	-8.45	25.33	-0.92
WA	-3.81	16.65	-0.3
WI†	-3.05	13.7	-0.24

* indicates a feasible solution; † indicates that this solution was over budget.

optimality of the returned solution within the time limit. Feasible solutions still provide insight into treatment facility distributions that would be more ideal than the current distribution. Table 3 shows that the feasible solutions have a positive impact on each population compartment, although this impact could be greater with optimal solutions.

We also identify whether the solution for a state is over budget by looking at the value of parameter h which indicates how many more treatment facilities in addition to N were necessary for the MIP to yield an optimal or feasible solution. If $h > 0$, the solution is over budget, and if $h = 0$, the solution stays within budget. Table 4 shows the value of

Table 4: Number of facilities over budget (h) for states with over budget solutions.

State	AL	AR	GA	IA	KS	KY	LA	MA	MN	MO	NE	NJ	NM	NV	OK	TN	TX	VA	WI
h	29	29	70	61	67	18	18	5	32	12	77	1	3	10	31	30	170	49	4

h for each state whose MIP yields an over budget solution. In particular, Texas, Nevada, Georgia, Kansas, and Iowa need to obtain significantly more funding at the state level for opioid treatment facility expansion. Texas’s solution is the most over budget, allocating 170 more facilities than the state has the budget for. This is likely because Texas has many counties, most of which currently have 0 treatment facilities offering MAT. The solver needed to allocate at least 1 treatment facility to every county, which caused the solution to be over budget. Figure 7 shows that the solution to the Texas MIP allocates 1 additional treatment

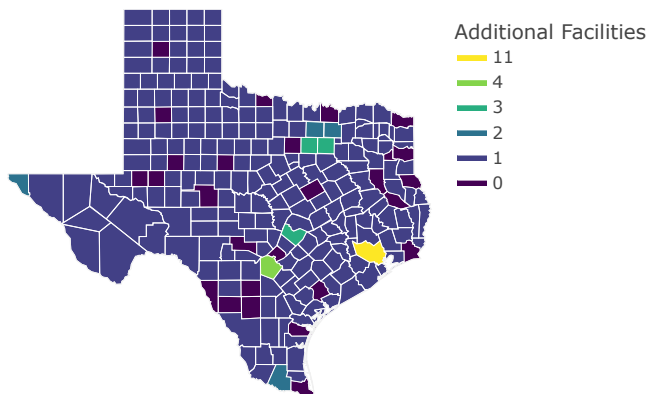


Figure 7: Amount of additional treatment facilities that should be opened in each county determined by the Texas MIP solution.

facility to the majority of counties, which aligns with our explanation. States with a larger number of counties tend to have more counties that currently have 0 treatment facilities, which leads to over budget MIP solutions. In turn, states that have over budget solutions likely have greater percent changes related to each compartment value than they would have had if their solutions were within budget. As shown in Figure 6, the within-budget solutions

still on average decrease the number of people with OUD by $5.07 \pm 1.011\%$, increase the number of people getting treatment by $18.47 \pm 4.058\%$, and decrease the number of opioid-related deaths by $0.39 \pm 0.070\%$ after 2 years.

5 Conclusions

In this work, we develop a novel optimization approach that considers complex opioid epidemic dynamics to compute optimal opioid treatment facility locations and treatment budget distributions. The integration of a prescriptive MIP with a dynamical model gives us the ability to show the direct impact of the MIP solutions on epidemic dynamics, and helps the MIP yield solutions that maximize positive impact on population health measures described by the epidemic model.

Our compartmental ODE model formulation expands on previous models of the opioid epidemic by including additional representative compartments: an illicit opioid use population compartment and a deceased compartment. This helps us capture illicit opioid use dynamics and incorporate cumulative overdose death data into our model more concretely. Although there have been previous state- and national-level compartmental ODE models of the opioid epidemic defined in the literature, no past work estimates unique parameters for almost every US state. We are able to capture the differences in the dynamics of the epidemic between states and interpret these differences through the model parameters. This helps us more accurately see the impact of our proposed interventions that affect each set of model parameters.

We then compute optimal resource allocation interventions using our MIP formulation for each state and quantify the differential impact of the varying state-level MIP solutions. Our MIP solutions provide insight into the additional number of treatment facilities that should be in each county to minimize opioid-related deaths and OUD prevalence under budgetary constraints. The solutions also indicate how much of a limited treatment budget per time period should be allocated to each county. Importantly, we prioritize social vulnerability within our MIPs so that their proposed solutions make the distribution of treatment facilities more socioeconomically equitable within states. In order to ensure MIP feasibility, we allow some solutions to be “over budget” in terms of the number of treatment facilities that can be opened within a particular state. We find that certain states like Oklahoma, Alabama, and Nevada should consider obtaining more funding to address opioid treatment facility expansion.

Our approach has limitations. Even though neural ODEs can deal with irregularly-sampled time series data, data quality and availability was a challenge when estimating parameters for our compartmental models. Having improved and more refined data related to illicit opioids, particularly fentanyl use, could benefit the quality of the parameter estimation, but we still have established that a neural ODE framework can be used for this application. We also estimated the overall budget and some of the parameters involved in our MIPs. Nevertheless, these parameters can be updated by decision-makers who have more insight into the parameters’ actual values. Additionally, we could not capture certain populations

within our epidemiological model, like individuals who started out using illicit opioids rather than transitioning from prescription opioids.

However, our integrated approach is general enough to accommodate possible epidemiological model variations, different MIP formulations, and different interventions. For instance, if policy-makers are interested in how to optimize the distribution of the overdose-reversing drug naloxone, they could still use this approach; the intervention would just affect a different compartmental model parameter (which would likely be μ , the death rate of addicts). In addition, it could also be possible to make decisions for combined interventions that affect several model parameters (*i.e.*, optimizing the naloxone distribution, opioid treatment facility locations, and treatment budget allocations).

Our contributions are two-fold: (1) we provide interpretable parameters which quantify the differences between the opioid epidemic dynamics of different states through parameter estimation with neural ODEs, and (2) we formulate a novel MIP approach that proposes more equitable, optimal solutions for opioid treatment facility location and treatment budget allocation. We show that the proposed solutions could have a positive impact, even in the short term, on population health measures. To our knowledge, the approach of integrating a predictive dynamical model with a prescriptive optimization problem has not been explored within opioid epidemic modeling and policy-related literature. In contrast from previous work, our approach directly provides concrete and actionable decisions based on real-world data regarding opioid treatment allocation. Combined with easy-to-use graphical visualization tools, this approach could be used by policy-makers to inform decision-making regarding the opioid epidemic in the future.

Appendix A Compartmental Model Initial Condition

Since data was not available for every compartment in 1999, we calculated most of the initial compartment values for each state based on previous research. For the P compartment, a CDC Vital Signs report [Paulozzi et al., 2011] indicated that the sales of prescription opioids in 2010 were 4 times those in 1999, which we used as a proxy for the comparison between the number of people using prescription opioids in 1999 and 2010 respectively. The value for P in 2010 was divided by 4 to get the initial P compartment value for each state. For the I compartment, we performed calculations based on data that stated that the annual average rate of past-year heroin use was 1.6 per 1000 persons in 2002–2004 nationally compared to 2.6 per 1000 persons in 2011–2013 nationally [Jones et al., 2015]. We approximated the initial I compartment value by multiplying the value for I in 2016 (the earliest year of data we had for this compartment) by 1.6/2.6 for each state. We assumed that the illicit users population did not change much from 1999–2002 and 2013–2016. For the A compartment, we utilized data from a study that indicated the prevalence of prescription opioid use disorder was 0.6% in 2003 compared to 0.9% in 2013 [Han et al., 2015]. We multiplied the value for A in 2016 (the earliest year of data we had for this compartment) by 6/9 for each state. This resulting value was used as the initial A compartment value, as we assumed the addicted population did not change much between 1999–2003 and 2013–2016. For the R compartment, we multiplied the data from 2000 by 0.75 to get the initial value for each state. The multiplier was determined based on the data trend. For the D compartment, we used the data we had for 1999 as the initial D compartment value for each state. The initial S compartment value was calculated based on data from the other 5 compartments and the populations of each US state in 1999.

Appendix B Reformulation of State-Level MIP

To ensure that our state-level MIP can be solved by Gurobi, we reformulate the problem to have at most quadratic constraints and a linear objective. We add new decision variables u_i , v_i , and z_i for all $i \in C$. The u_i 's and v_i 's are defined to reformulate the 1-norm terms in the objective. The z_i 's are continuous variables that are defined to turn the constraint where we divide two decision variables into a quadratic constraint. We have the expression \bar{d}_{ik}/dx_i , and we define $z_i = 1/x_i$ by adding the constraint $x_i \cdot z_i = 1$ for all $i \in C$. We reformulate the expression as $\bar{d}_{ik}z_i/d$. We bound x_i such that $x_i \in [1, N]$. Each county should have at least one treatment facility offering MAT, and N is the maximum number of facilities that can be opened within the state. We also define constants w_k for all $k \in \mathcal{K}$ to linearize the sum of infinity norms objective term, and a constant h to linearize the final objective term.

We can write the resulting problem as follows:

$$\begin{aligned}
& \text{minimize } D_K + \lambda_A \sum_{k=0}^K (A_k) + \lambda_{\text{pr}} \sum_{i=1}^C u_i + \lambda_{\text{SVI}} \sum_{i=1}^C v_i + \lambda_{\text{Pop}} \sum_{k=0}^K w_k + \lambda_{\text{inf}} h \\
& \text{subject to } \sum_{i=1}^C x_i - N \leq h, \quad 0 \leq h \\
& \quad x_i \geq n_i, \quad x_i \cdot z_i = 1, \quad \forall i \in \mathcal{C} \\
& \quad \sum_{i=1}^C \bar{d}_{ik} \leq d_k, \quad \forall k \in \mathcal{K} \\
& \quad -u_i \leq x_i - \frac{\text{pr}_i}{\sum_{i=1}^C \text{pr}_i} N \leq u_i, \quad \forall i \in \mathcal{C} \\
& \quad -v_i \leq x_i - \frac{\text{SVI}_i}{\sum_{i=1}^C \text{SVI}_i} N \leq v_i, \quad \forall i \in \mathcal{C} \\
& \quad -w_k \leq \bar{d}_{ik} - \frac{\text{Pop}_i}{\sum_{i=1}^C \text{Pop}_i} d_k \leq w_k, \quad \forall i \in \mathcal{C}, k \in \mathcal{K} \\
& \quad S_{k+1} = S_k + (\epsilon P_k + \delta R_k - \alpha S_k) \Delta, \quad k = 1, \dots, K-1 \\
& \quad P_{k+1} = P_k + (\alpha S_k - (\epsilon + \gamma + \beta) P_k) \Delta, \quad k = 1, \dots, K-1 \\
& \quad I_{k+1} = I_k + (\beta P_k - \phi I_k) \Delta, \quad k = 1, \dots, K-1 \\
& \quad A_{k+1} = A_k + (\gamma P_k + \sigma R_k + \phi I_k - (\zeta + \ell_k) A_k - \mu A_k) \Delta, \quad k = 1, \dots, K-1 \\
& \quad R_{k+1} = R_k + ((\zeta + \ell_k) A_k - (\delta + \sigma) R_k) \Delta, \quad k = 1, \dots, K-1 \\
& \quad D_{k+1} = D_k + (\mu A_k) \Delta, \quad \forall k \in \mathcal{K} \\
& \quad x_i \in \mathbf{Z}, \quad x_i \in [1, N], \quad k = 1, \dots, K-1 \\
& \quad \bar{d}_{ik}, u_i, v_i, z_i, w_k, S_k, P_k, I_k, A_k, R_k, D_k \geq 0, \quad \forall i \in \mathcal{C}, k \in \mathcal{K},
\end{aligned}$$

where we define

$$\ell_k = \frac{\sum_{i=1}^C d^{-1}(x_i - n_i) \bar{d}_{ik} z_i}{A_k}.$$

This mixed-integer non-convex optimization problem is solved by Gurobi as a bilinear problem.

Appendix C MIP Hyperparameter Tuning

We tune the λ_{inf} hyperparameter for each state-level MIP, to account for the fact that the magnitude of each MIP differs (*i.e.*, each state has a different number of counties and a different population magnitude). We set λ_{inf} to a large enough value to ensure that the MIP solver can find feasible solutions as well as minimize the amount that a solution is over budget. In this way, λ_{inf} acts as a soft-constraint penalty parameter, since it is a large parameter set in order to help the solver find feasible solutions. We estimate this parameter

specifically for certain states, which involves testing a range of parameter values within the range [100, 500]. After tuning, we set $\lambda_{\text{inf}} = 475$ for Michigan, Florida, and Washington; $\lambda_{\text{inf}} = 500$ for Illinois; $\lambda_{\text{inf}} = 276$ for New Jersey; $\lambda_{\text{inf}} = 175$ for Maryland; $\lambda_{\text{inf}} = 123$ for Massachusetts, and $\lambda_{\text{inf}} = 450$, otherwise.

Appendix D Tables and Figures

Table 5 shows the exact values of the parameters we estimate using the neural ODE model for each state. Figure 8 shows how the training loss evolves over 20000 iterations of training for the New York neural ODE model. The loss decreases and eventually flattens off as the number of iterations increases. The final loss is less than a magnitude of 10^{-4} . This indicates that the model has found the best possible parameter values. We use the results from New York to show an illuminating example of how our models tend to fit to the data.

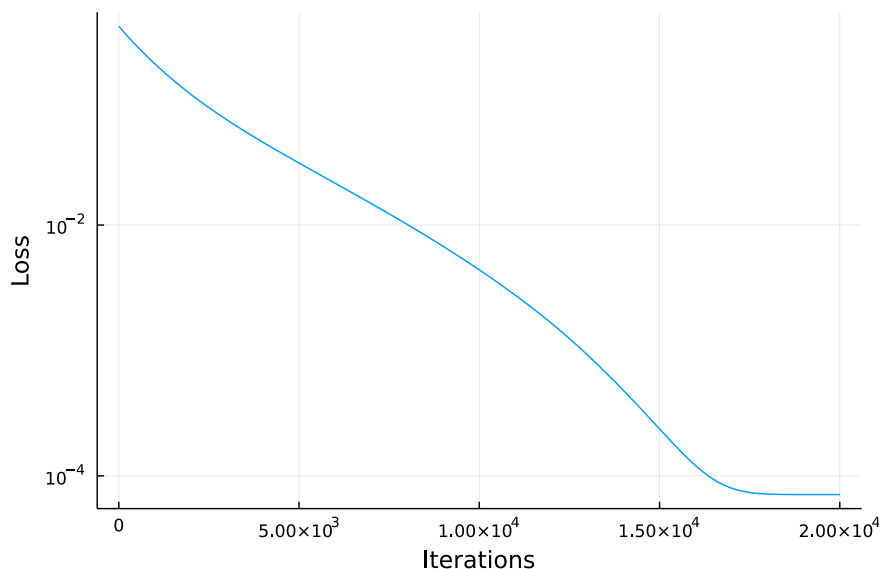


Figure 8: New York neural ODE model loss function trajectory for 20000 training iterations.

Table 5: Estimated parameters for each US state.

State	ϕ	ϵ	β	ζ	μ
AL	0	1.307	0.0000925	0.2871	0.00788
AR	0	1.464	0.001	0.2361	0.01636
AZ	0	2.291	0	0.2693	0.00885
CA	0	3.57	0	0.2731	0.00845
CO	0	2.724	0	0.2132	0.0093
CT	0.04267	2.769	0.004863	0.4428	0.00978
DE	0.03041	1.938	0.003776	0.2426	0.00571
FL	0	2.354	0	0.1843	0.0099
GA	0	2.112	0	0.3405	0.01338
HI	0	3.99	0.000394	0.185	0.01035
IA	0	2.765	0.001285	0.1064	0.00969
IL	0	2.973	0.001353	0.2537	0.01157
IN	0	1.8	0.000142	0.2515	0.00761
KS	0	2.137	0.000574	0.3308	0.01461
KY	0	1.458	0	0.1902	0.00818
LA	0	1.606	0	0.3065	0.01038
MA	0.0459	3.027	0.003099	0.2823	0.00517
MD	0.05173	2.74	0.004663	0.5151	0.01392
ME	0.06146	2.21	0.003482	0.2867	0.00458
MI	0	1.928	0.000784	0.2571	0.01402
MN	0	3.412	0	0.4333	0.01297
MO	0	2.03	0.00014	0.2512	0.01486
NC	0	1.972	0.000378	0.2718	0.01356
NE	0	2.689	0.000172	0.2757	0.01276
NH	0	2.353	0	0.1853	0.00933
NJ	0.01966	3.186	0.003131	0.1817	0.00676
NM	0.01186	2.524	0.001433	0.3059	0.02149
NV	0	1.967	0	0.1622	0.01304
NY	0.05511	3.916	0.005029	0.4383	0.01064
OH	0	2.006	0	0.1098	0.00793
OK	0	1.556	0	0.3297	0.02198
OR	0	1.969	0	0.2563	0.0084
PA	0	2.361	0.001773	0.2184	0.00812
RI	0	2.435	0.000279	0.4883	0.00889
SC	0	1.831	0.00000316	0.2997	0.01279
TN	0	1.388	0	0.3383	0.01268
TX	0	2.721	0	0.378	0.01317
UT	0	2.181	0	0.2526	0.01542
VA	0	2.565	0	0.1838	0.01007
VT	0.1004	3.187	0.01647	0.2776	0.01075
WA	0	2.349	0	0.2085	0.00887
WI	0	2.621	0.000607	0.2131	0.0123

Note: We treated all parameters that were less than 10^{-7} as approximately 0.

References

- Solmaz Amiri, Michael G. McDonell, Justin T. Denney, Dedra Buchwald, and Ofer Amram. Disparities in Access to Opioid Treatment Programs and Office-Based Buprenorphine Treatment Across the Rural-Urban and Area Deprivation Continua: A US Nationwide Small Area Analysis. *Value in Health*, 24(2): 188–195, 2020.
- Ascension Recovery Services. The Cost of Opening an Addiction Treatment Center. <https://www.ascensionrs.com/the-climb/the-cost-of-opening-an-addiction-treatment-center>, 2019. Accessed on 2022-03-25.
- Nathan A. Battista, Leigh B. Percy, and W. Christopher Strickland. Modeling the Prescription Opioid Epidemic. *Bulletin of Mathematical Biology*, 105:2258–2289, 2019.
- Jesse C. Baumgartner and David C. Radley. The Spike in Drug Overdose Deaths During the COVID-19 Pandemic and Policy Options to Move Forward. <https://www.commonwealthfund.org/blog/2021/spike-drug-overdose-deaths-during-covid-19-pandemic-and-policy-options-move-forward>, 2021. Accessed on 2022-03-21.
- Dimitris Bertsimas, Vassilis Digalakis Jr, Alexander Jacquillat, Michael Lingzhi Li, and Alessandro Previero. Where to locate COVID-19 mass vaccination facilities? *Naval Research Logistics*, page 1–20, 2021.
- Centers for Disease Control. CDC WONDER - About Multiple Cause of Death, 1999-2019. <https://wonder.cdc.gov>, 2019. Accessed on 2021-10-28.
- Centers for Disease Control. Drug Overdose Deaths. <https://www.cdc.gov/drugoverdose/deaths/index.html>, 2021a. Accessed on 2021-09-08.
- Centers for Disease Control. U.S. Opioid Dispensing Rate Maps. <https://www.cdc.gov/drugoverdose/rxrate-maps/index.html>, 2021b. Accessed on 2021-10-28.
- Centers for Disease Control. Opioids: Understanding the Epidemic. <https://www.cdc.gov/opioids/basics/epidemic.html>, 2021c. Accessed on 2021-09-08.
- Centers for Disease Control, National Center for Health Statistics. National Health and Nutrition Examination Survey, 1999-2018. <https://wwwn.cdc.gov/nchs/nhanes/>, 2019. Accessed on 2022-01-22.
- Centers for Disease Control/Agency for Toxic Substances and Disease/Geospatial Research, Analysis, and Services Program. CDC/ATSDR Social Vulnerability Index Database US. https://www.atsdr.cdc.gov/placeandhealth/svi/data_documentation_download.html, 2021. Accessed on 2021-09-02.
- Centers for Medicare and Medicaid Services. Opioid Treatment Programs (OTPs) Medicare Billing & Payment. <https://www.cms.gov/files/document/otp-billing-and-payment-fact-sheet.pdf>, 2021. Accessed on 2022-03-25.
- Qiushi Chen, Marc R. Larochelle, Davis T. Weaver, Anna P. Lietz, Peter P. Mueller, Sarah Mercaldo, Sarah E. Wakeman, Kenneth A. Freedberg, Tiana J. Raphel, Amy B. Knudsen, Pari V. Pandharipande, and Jagpreet Chhatwal. Prevention of Prescription Opioid Misuse and Projected Overdose Deaths in the United States. *JAMA Network Open*, 2(2):e187621–e187621, 2019.
- Ricky T. Q. Chen, Yulia Rubanova, Jesse Bettencourt, and David Duvenaud. Neural Ordinary Differential Equations, 2018. URL <https://arxiv.org/abs/1806.07366>.

- Iain Dunning, Joey Huchette, and Miles Lubin. JuMP: A modeling language for mathematical optimization. *SIAM Review*, 59(2):295–320, 2017.
- Beth Han, Wilson M. Compton, Christopher M. Jones, and Rong Cai. Nonmedical Prescription Opioid Use and Use Disorders Among Adults Aged 18 Through 64 Years in the United States, 2003-2013. *JAMA*, 314(14):1468–1478, 10 2015.
- Christopher M. Jones, Joseph Logan, R. Matthew Gladden, and Michele K. Bohm. Vital Signs: Demographic and Substance Use Trends Among Heroin Users — United States, 2002–2013. *MMWR*, 64(26):719–725, 2015.
- William Ogilvy Kermack, A. G. McKendrick, and Gilbert Thomas Walker. A contribution to the mathematical theory of epidemics. *Proceedings of the Royal Society of London*, 115(772):700–721, 1927.
- Stephen E. Lankenau, Michelle Teti, Karol Silva, Jennifer Jackson Bloom, Alex Harocopos, and Meghan Treese. Initiation into prescription opioid misuse amongst young injection drug users. *International Journal of Drug Policy*, 23(1):37–44, 2012.
- Michael Lingzhi Li, Hamza Tazi Bouardi, Omar Skali Lami, Thomas A. Trikalinos, Nikolaos Trichakis, and Dimitris Bertsimas. Forecasting COVID-19 and Analyzing the Effect of Government Interventions. *Operations Research*, 0(0):null, 2022.
- RP Mattick, C Breen, J Kimber, and M Davoli. Buprenorphine maintenance versus placebo or methadone maintenance for opioid dependence. *Cochrane Database of Systematic Reviews*, (2), 2014.
- Pradip K. Muhuri, Joseph C. Gfroerer, and M. Christine Davies. Associations of Nonmedical Pain Reliever Use and Initiation of Heroin Use in the United States. *CBHSQ Data Review*, 2013.
- Suzanne Murrin. States’ Use of Grant Funding for a Targeted Response to the Opioid Crisis. <https://oig.hhs.gov/oei/reports/oei-BL-18-00460.pdf>, 2020. Accessed on 2022-03-25.
- National Institute of Drug Abuse. Medications to Treat Opioid Use Disorder Research Report. <https://nida.nih.gov/publications/research-reports/medications-to-treat-opioid-addiction/overview>, 2018. Accessed on 2021-09-08.
- National Institute on Drug Abuse. Opioid Overdose Crisis. <https://nida.nih.gov/drug-topics/opioids/opioid-overdose-crisis>, 2021. Accessed on 2022-03-27.
- Leonard J. Paulozzi, Christopher M. Jones, Karin A. Mack, and Rose A. Rudd. Vital Signs: Overdoses of Prescription Opioid Pain Relievers-United States, 1999-2008. *MMWR*, 60(43):1487–1492, 2011.
- Allison L. Pitt, Keith Humphreys, and Margaret L. Brandeau. Modeling Health Benefits and Harms of Public Policy Responses to the US Opioid Epidemic. *American Journal of Public Health*, 108(10):1394–1400, 2018.
- Christopher Rackauckas and Qing Nie. DifferentialEquations.jl – A Performant and Feature-Rich Ecosystem for Solving Differential Equations in Julia. *The Journal of Open Research Software*, 5(1), 2017.
- Christopher Rackauckas, Mike Innes, Yingbo Ma, Jesse Bettencourt, Lyndon White, and Vaibhav Dixit. DiffEqFlux.jl - A Julia Library for Neural Differential Equations. *CoRR*, abs/1902.02376, 2019.
- Isabelle J Rao and Margaret L Brandeau. Optimal allocation of limited vaccine to control an infectious disease: Simple analytical conditions. *Math. Biosci.*, 337(108621):108621, July 2021.

- Isabelle J. Rao, Keith Humphreys, and Margaret L. Brandeau. Effectiveness of Policies for Addressing the US Opioid Epidemic: A Model-Based Analysis from the Stanford-Lancet Commission on the North American Opioid Crisis. *The Lancet Regional Health – Americas*, 3, Nov 2021. ISSN 2667-193X.
- Anuj Shah, Corey J Hayes, and Bradley C Martin. Characteristics of initial prescription episodes and likelihood of long-term opioid use—United States, 2006–2015. *MMWR*, 66(10):265, 2017.
- Substance Abuse and Mental Health Services Administration. Behavior Health Treatment Services Locator. <https://findtreatment.samhsa.gov/locator>, 2022. Accessed on 2022-03-21.
- United States Census Bureau. County Population Totals: 2010-2019. <https://www.census.gov/data/datasets/time-series/demo/popest/2010s-counties-total.html>, 2021. Accessed on 2022-03-25.
- U.S. Department of Health and Human Services. HHS Grant Funding to Address the U.S. Opioid Crisis. <https://www.hhs.gov/opioids/about-the-epidemic/opioid-crisis-statistics/opioids-grants-dashboard/index.html>, 2020. Accessed on 2022-03-25.
- U.S. Department of Health and Human Services, Substance Abuse and Mental Health Services Administration, Center for Behavioral Health Statistics and Quality. National Survey on Drug Use and Health. <https://www.samhsa.gov/data/data-we-collect/nsduh-national-survey-drug-use-and-health>, 2019. Accessed on 2021-09-08.
- U.S. Department of Health and Human Services, Substance Abuse and Mental Health Services Administration, Center for Behavioral Health Statistics and Quality. National Survey of Substance Abuse Treatment Services. <https://www.samhsa.gov/data/data-we-collect/n-ssats-national-survey-substance-abuse-treatment-services>, 2021. Accessed on 2021-09-08.
- Emma White and Catherine Comiskey. Heroin epidemics, treatment and ODE modelling. *Mathematical Biosciences*, 208(1):312–324, 2007.
- Karen Willcox and Qiqi Wang. 16.90 Computational Methods in Aerospace Engineering, Spring 2014 - The Forward Euler Method. Massachusetts Institute of Technology: MIT OpenCourseWare, 2014. Accessed on 2022-09-05, License: Creative Commons BY-NC-SA.
- Gregory S. Zaric and Margaret L. Brandeau. Dynamic resource allocation for epidemic control in multiple populations. *Mathematical Medicine and Biology: A Journal of the IMA*, 19(4):235–255, 12 2002. ISSN 1477-8599.